Crystal structure, IR, Raman and UV-Vis studies of

$[Co(H_2P_2O_7)_2(H_2O)_2][(CH_3)_3C\text{-}NH_3)]_2{\cdot}2H_2O$

Aziz Alaoui Tahiri [1], Brahim El Bali [2,*], Mohammed Lachkar [3], Claire Wilson [4], David Bauer [5] and Christoph Haisch [5]

[1] Laboratoire de Chimie Analytique et Moléculaire (LCAM), Faculté Polydisciplinaire-Safi Université Cadi Ayyad, Route Sidi Bouzid B.P. 4162 Safi, Morocco.

[2] Independent Scientist, Oujda, Morocco, ORCID: 0000-0001-6926-6286; Email: b_elbali@yahoo.com

[3] Engineering Laboratory of Organometallic and Molecular Materials, Faculty of Sciences, University Sidi Mohamed Ben Abdellah, Po. Box 1796 (Atlas), 30000 Fez, Morocco.

[4] University of Glasgow, School of Chemistry, Joseph Black Building, Glasgow, G12 8QQ United Kingdom.

[5] Chair of Analytical Chemistry, Technical University of Munich, Elisabeth-Winterhalter-Weg 6, D-81377 Munich, Germany.

Abstract

$[Co(H_2P_2O_7)_2(H_2O)_2][(CH_3)_3C\text{-}NH_3]_2\cdot 2H_2O$, a new organically templated dihydrogen-pyrophosphate compound, was synthesized and characterized. The crystal structure was determined using single crystal X-ray diffraction data; $[Co(H_2P_2O_7)_2(H_2O)_2][(CH_3)_3C\text{-}NH_3]_2\cdot 2H_2O$ crystallizes in orthorhombic space group Cmce (n 64), Z = 4, a= 11.9 642(10), b= 9.1565(8), c= 24.488(2), V = 2682.7(4) Å3. Final agreement factors for the refined structure model are R/Rw (%) were 3.96/9.12. The open framework of $[Co(H_2P_2O_7)_2(H_2O)_2][(CH_3)_3C\text{-}NH_3]_2\cdot 2H_2O$ might be described as phosphor-metallic slabs, made of isolated octahedrons $[Co(H_2P_2O_7)_2(H_2O)_2]$, which interact through intra-slab H-bonds, while inter-slabs H-bonds ensure the interactions of neighbouring slabs. The inter-slabs host the counter ion $[(CH_3)_3C\text{-}NH_3)]^+$ ions and H_2O molecules. Raman and FTIR spectra of the newly synthesized compound confirm the structural data obtained by X-Ray diffraction. The complementary information about vibrational modes prove the presence and the coordination of the phosphates as well as the organic moieties. UV-Vis spectrophotometry provide evidence of d-d transitions that are typically found in octahedral Co(II) compounds. In the visible region, the electronic spectrum is dominated by a well resolved strong band at 505 nm assigned to the spin allowed transition $^4T_{1g}(F) \rightarrow {}^4T_{1g}(P)$, and a shoulder at about 460 nm which is assigned to $^4T_{1g}(F) \rightarrow {}^4A_{2g}(F)$ transition that is manifold splitted due to multiplet coupling.

Keywords: Hybrid phosphate; Crystal structure; IR; Raman; UV-Visible.

I- Introduction

Hybrid materials are the most attractive competitors of multifunctional materials due to their rich topology and applications diversity in fields like catalysis, ion exchange, adsorption, magnetism and photochemistry [1-9]. Among the multipurpose characteristics of the multifunctional materials; structure, optical and magnetic properties accurately represent a huge challenge for the scientists of modern technology owing to their encouraging applications such as high-density information storage, spintronics, and solar cell conversation [10, 11].

Besides, large number of studies have been devoted to the preparation of new organic inorganic metal phosphates, which combine the robustness of phosphate group and the versatility of organic template giving rise to various architectures and excellent properties [12-17]. In contrast to numerous hybrid organic inorganic metal phosphates and phosphites reported [18-22], the structural chemistry of homologous pyrophosphates is relatively rare. Within our research group, we published the synthesis and crystal structure of $(NH_3(CH_2)_2NH_3)_2[Me(HP_2O_7)_2 \cdot 2H_2O]$ [Me = Mg [23], Co, Ni [24] and $Ln_2(NH_2(CH_2)_2NH_2)(HP_2O_7)_2 \cdot 4H_2O$ (Ln=Eu, Tb, Er) [25]. A novel 3-D manganese open-framework, $[NH_3(CH_2)_2NH_3][MnP_2O_7]$ has been synthesized under ionothermal conditions and characterized by single crystal X-ray diffraction [26]. The bridged binuclear complex, $[Co_2(phendione)_4(P_2O_7)] \cdot nH_2O$ was prepared, structurally and magnetically characterized [27].

Our previous work was focused on the synthesis and characterizations of acidic metal pyrophosphates. We have prepared, via an easy and eco-friendly wet chemistry route, a series of mixed dihydrogenpyrophosphates $A_2M(H_2P_2O_7)_2 \cdot xH_2O$ [A is an alkali metal, Tl or ammonium and M a divalent 3d transition metal (including Zn) or Mg] [28-37]. Encouraged by this strategy, we herein report the synthesis and characterizations of a new organically templated dihydrogenpyrophosphate compound with general chemical formula

$[Co(H_2P_2O_7)_2(H_2O)_2][(CH_3)_3C\text{-}NH_3]_2 \cdot 2H_2O$, namely Tert-butyl amine dihydrogenpyrophosphate cobalt(II) dihydrate. We present the structural characterization by single-crystal X-ray diffraction, Fourier transform FTIR spectroscopy, FT Raman spectroscopy and UV-vis absorption spectroscopy.

II. Experimental

II.1 Synthesis

The $[Co(H_2P_2O_7)_2(H_2O)_2][(CH_3)_3C\text{-}NH_3]_2 \cdot 2H_2O$ crystals were obtained from a mixture of $Na_4P_2O_7$ (450mg, 1mmol) and $Co(NO_3)_2 \cdot 6H_2O$ (146.8mg, 0.5mmol), dissolved in few ml of diluted HCl (0.75mL of HCl 0.1M), in the presence of (CH3)3CNH2·HCl (110.5mg, 1mmol) as structure directing agent. The mixture was stirred for 2 h, then evaporation of solvent water was allowed for two weeks at room temperature. Prismatic crystals with edge-length up to 0.2 mm deposited at the end of this period. They were filtered off and washed with water - ethanol mixture (20:80).

II-2 Single crystal characterization

A single crystal of the title compound was selected for X-ray diffraction analysis. Data were collected at room temperature using a Bruker D8 VENTURE diffractometer [using Mo-Kα radiation (λ= 0.71073 Å)], equipped with a Photon II CPAD detector and an IμS 3.0 (dual Cu and Mo) microfocus sealed tube generator. Diffraction data were collected and processed using *APEX3* Ver. 2016.9-0 Bruker-AXS, 2016). The structures were solved using SHELXT [38] and refined using SHELXL [39] within OLEX2 [40]. All non-Hydrogen atoms were refined with anisotropic atomic displacement parameters. Hydrogen atoms were located in difference Fourier maps and refined freely except for the Me hydrogen atoms which were either placed in geometrically calculated positions and refined as part of a riding model, or as rigid rotor with isotropic adps at 1.5U(eq) of the parent carbon atom. A distance restraint was applied to the O4-H4 distance.

Details of the data collection and refinement are given in Table 1. The atomic coordinates are reported in Table 2, while Table 3 contains the basic geometrical data. The CIF has been deposited with the Cambridge Structure Database **CCDC 2008482**. The structural graphics were created using the software Diamond [41].

II-3 Spectroscopic characterizations

Raman spectra were acquired from different spots of several single crystals with a WITec Alpha 300R microscope (WITec GmbH, Ulm, Germany), equipped with a Cobolt DPL 532 nm solid state laser (Cobolt AB, Solna, Sweden) and a true-power module ensuring a stable laser power of 1 mW. In total, 13 spectra were recorded, each an average of three spectra measured again with an integration time of 5 s each. The spectral range covered is 150 to 3800 cm^{-1}. The laser light was focused onto the sample using a 20× objective (Zeiss EC Eipplan 20x/0.4; Carl Zeiss AG, Germany). The scattered Raman photons were collected in reflection mode and detected via a fiber-coupled spectrometer (UHTS 300, f/4, 300 mm focal length) including a 600 l/mm grating and a Newton 970 EMCCD camera (Andor Technology Ltd., Belfast, UK). Raman spectra were background corrected in MATLAB, version 2018b (The Mathworks Inc., Natick, United States) by means of the 'backcor' function, and normalized using the Euclidean norm.

For the acquisition of the FT-IR spectrum, a Thermo Fisher Nicolet 6700 FT-IR spectrometer (Thermo Scientific, Waltham, United States) was employed in attenuated total reflection (ATR) mode. After recording the background spectrum, enough crystals to cover the window of the Smart iTR sample stage were used. The spectrum was recorded averaging 16 scans with a resolution of 4 cm^{-1} and background subtraction was carried out by the OMNIC software.

To carry out UV-Vis spectrophotometry a spatula of the crystals was suspended in 1.5 mL MilliQ water (Merck KGaA, Darmstadt, Germany) in an Eppendorf tube and put in an ultrasound bath for 1 hour. The suspension was transferred into a polystyrene semi-micro cuvette (BRAND GmbH +

CO KG, Wertheim, Germany) and the absorbance spectrum was acquired on a Specord 250plus (Analytik Jena AG, Jena, Germany) from 250 to 1000 nm in steps of 5 nm.

III- Results and discussion

III-1 Crystal structure

Single crystal X-ray diffraction analysis reveals that the synthesized compound $[Co(H_2P_2O_7)_2(H_2O)_2][(CH_3)_3C\text{-}NH_3]_2\cdot 2H_2O$ crystallizes in the orthorhombic symmetry, space group Cmce (n 64). The asymmetric unit contains 0.25 of the formula unit of title compound, with a single crystallographically independent Co site, 0.5 $H_2P_2O_7$, one coordinated and free water position and 0.5 tButyl-ammonium cation. A formula unit is shown in Figure 1.

The open framework of $[Co(H_2P_2O_7)_2(H_2O)_2][(CH_3)_3C\text{-}NH_3]_2\cdot 2H_2O$ might be described as phosphor-metallic *ab*-parallel slabs, made of the octahedrons $[Co(H_2P_2O_7)_2(H_2O)_2]^{-2}$, $[(CH_3)_3C\text{-}NH_3)]^{+}$ and H_2O. In fact, the $[Co(H_2P_2O_7)_2(H_2O)_2]^{-2}$ anions engage, on one hand, a network of H-Bonds to connect to each other and thus define the phosphor-metallic slabs. The strongest H-bonds are O3--H1-O1 (1.975 Å) and O3--H4-O4 (1.715 Å) (Table 4). On the other hand, the slabs are linked through similar H-Bonds, i.e.: O1..H1-N1 (2.092 Å) and O3--H2-O2 (2.163 Å), via the hosted $[(CH_3)_3C\text{-}NH_3)]^{+}$ cations and H_2O molecules (Table 4, Figure 2).

The protonated $tBuNH_3^+$ amine, in its character of counter ion to balance the overall negative charge of the open framework, reside in the interlayers. It is linked to the phosphor-metallic slab via O...H---O bonds induced by the free water [$H_2O(2)$] and N...H---O from the $tBuNH_3^+$ ion. The Co(II) cation adopts an octahedral coordination geometry with four O atoms from two bidentate $H_2P_2O_7$ groups, the two remaining apices are aqua ligands. There are two crystallographically independent Co-O bond lengths (Table 3a) 2.058(2) Å to the apical water oxygen and 2.111(1) Å to the phosphate, in the same order as in homologous cobalt pyrophosphates like in $K_2Co(H_2P_2O_7)\cdot 2H_2O$ [28] and $Tl_2Co(H_2P_2O_7)\cdot 2H_2O$ [37].

The Co(II) cation occurs in distorted octahedral coordination (Table 3), its coordination sphere contains four O atoms from two bidentate $H_2P_2O_7$ acid pyrophosphate groups and the remaining two ones from water H_2O molecules. The equatorial plane around the Co atom is slightly distorted, with a chelate angle of 86.00(7)° and 94.00(7)° between the two ligands and a linear equatorial $O1_W$-Co1-$O1_W$ (Table 3). According to the formula $\Delta_{oct}= 1/6*\Sigma[(di-dm)/dm]^2$ [42, 43], the bond-length distortions for the Co atom amount $\sim 10^{-6}$ indicates indeed negligible distortions as to compare with the value reported in $[Co(H_2PO_2)(C_{12}N_4H_{16})]Cl_2$, $4.5\cdot 10^{-3}$ [44].

As expected, the pyrophosphate anion (Table 3b) displays three types of P-O distances, long distance d(P-$O_{bridging}$) 1.5785(10) Å corresponding to P-O bridging bonds, intermediate d(P-OH)= 1.542(2)Å involving hydroxyl group and short distances d(P-$O_{terminal}$) ~ 1.4966(13) Å and 1.4891(13) Å corresponding to external O atoms. The pyrophosphate group adopts a nearby eclipsed conformation, with a dihedral angle of 5.3°with the bridging angles ∠(P,O,P) of 136.5° , also to compare with the values reported in known acidic pyrophosphates [23-37].

III-2 Vibrational study

IR and Raman spectra of $[Co(H_2P_2O_7)_2(H_2O)_2][(CH_3)_3C\text{-}NH_3]_2\cdot 2H_2O$ are depicted in Figures 3 and 4, respectively. The noisy I. R. spectrum might be maybe due to an overwhelmed of the room with CO_2 and H_2O or simply to apodization settings. The assignment of bands is made by correlation with vibrations characteristics of the phosphate group, organic amine and water molecules [45-49]. However, overlapping of various vibrations, potentially present in the same spectral range, render exact assignment of all the bands in both IR and Raman spectra difficult. The IR spectrum showed characteristic [P—O—P] stretches at approximately 910 and 750 cm^{-1}. The presence of the organic t-But molecule was indicated by the Raman peaks in the 2800-3000 cm^{-1} region. Moreover, In the high frequencies region 2000-3500 cm^{-1}, the vibrations corresponding to the O-H, N-H, and C-H stretching modes

should appear. In fact, weak bands around 3500 and 3480 cm^{-1} are caused by the stretching vibrations of water molecules, this is also revealed by the Raman peak at 3466 cm^{-1}. Symmetric and asymmetric stretching vibrations of the amino group result in weak bands in 3200-3500 cm^{-1} region. The appearance of peaks around 3300 cm^{-1} in the title compound is presumably due to the presence of extensive intermolecular H-bonding involving OH groups among water molecules coordinated to the Co(II) ions. Generally, the hydroxyl or amino group in a condensed phase might be involved in extensive intermolecular hydrogen bonding with a broad band appearing in the region 3200-3500 cm^{-1}. The 2800-3000 cm^{-1} region comprises well defined Raman peaks corresponding to the asymmetric and symmetric C-H vibrations characteristic of aliphatic CH_3 group. The additional Raman peaks at 2880 and 2780 cm^{-1} can be assigned to combination and overtone of CH_3 deformation modes. The I.R doublet around 2400 cm^{-1} is due to N-H^+ stretch of the amino group as this region is typically due to acidic and hydrogen-bonded hydrogen atom [45].

The bands occurring in the region 1660-1200 cm^{-1} correspond to all fundamental vibrations, related with angular distortions such as bending and stretching vibrations, involving the OH, NH_3 and CH_3 groups. N-H deformation are found in the region 1660-1520 cm^{-1}, while characteristic C-H deformation result in moderate IR band and weak to moderate Raman peaks in the 1500-1250 cm^{-1} region. We note also the presence of other bands in the 1250-1200 cm^{-1} region which can be assigned to the CC_3 skeletal stretching and vibration modes of C_3C-N moieties [45]. The strong IR absorption band at 1180 cm^{-1} is assigned to the asymmetric stretching of PO_3 group $\nu_{as}(PO_3)$, while the most intense Raman peak at 1054 cm^{-1} and the medium IR band at 1010 cm^{-1} are attributed to the $\nu_s(PO_3)$ symmetric stretching of PO_3 group [24]. For the behavior of the POP bridge vibrations, they always occur at lower frequency than the terminal P–O stretching modes [50]. The

intense I. R. band and the medium Raman peak situated at 910 cm^{-1} and 931 cm^{-1}, respectively are assigned to the asymmetric bridge vibrations ν_{as}(POP). While, the intense Raman peak and the weak I.R band observed at 736 cm^{-1} and are due to symmetric ν_s(POP) vibrations. The rocking and deformation modes δPO_3 and ρPO_3 are observed in the range between 600 and 400 cm^{-1}.

III-3 Absorption spectrum

The UV-Vis spectrum of $[Co(H_2P_2O_7)_2(H_2O)_2][CH_3)_3C\text{-}NH_3)_2]\cdot 2H_2O$ (Figure 5) exhibits an absorption bands in the ultraviolet region at 290 nm, which can be assigned to allowed charge transfer transitions, as no d-d excitations are expected to give rise to such high energy features. In the visible region, the electronic spectrum is dominated by a well resolved strong band at 505 nm assigned to the spin allowed transition $^4T_{1g}(F) \rightarrow {}^4T_{1g}(P)$, and a shoulder at about 460 nm which is assigned to $^4T_{1g}(F) \rightarrow {}^4A_{2g}(F)$ transition that is manifold splitted due to multiplet coupling [51]. In fact, Cobalt complexes exhibit absorption in the visible region around 530–570 nm and 730–760 nm corresponding to *d-d* transitions [52]. The observed d-d transitions, typical for Co(II) in octahedral coordination geometry, justify the pink color of the crystal.

IV Conclusions

Crystals of the hybrid acid pyrophosphate $[Co(H_2P_2O_7)_2(H_2O)_2][(CH_3)_3C\text{-}NH_3]_2\cdot 2H_2O$ were successfully synthesized via a wet chemistry route, in the presence of tert-butyl amine $[(CH_3)_3C\text{-}NH_3]_2\cdot 2H_2O$ as a structure directing agent. The title compound crystallizes with orthorhombic symmetry (S. G.: Cmce), with the cell parameters: a= 11.9 642(10), b= 9.1565(8), c= 24.488(2), V = 2682.7(4) $Å^3$. The final residual factors of the refined structure model R/Rw were 3.96% / 9.12%.

The open framework of the title compound consists in phosphor-metallic slabs, made of isolated octahedrons $[Co(H_2P_2O_7)_2(H_2O)_2]$, which interact through intra-slab H-bonds, while inter-slabs H-bonds ensure the interactions of neighbouring slabs, which host the counter ion $[(CH_3)_3C\text{-}NH_3)]^+$ ions and H_2O molecules. Characterizations were completed with complementary vibrational spectroscopic methods, FT-IR and Raman spectroscopy, which allowed the assignment of bands based on correlation with vibrations characteristics of the phosphate group, organic amine and water molecules. UV-Vis spectrum confirms a d-d transition typically for Cobalt(II) compounds and complete an extensive investigation of the new compound. In the visible region, the electronic spectrum is dominated by a well resolved strong band at 505 nm assigned to the spin allowed transition $^4T_{1g}(F) \rightarrow {}^4T_{1g}(P)$, and a shoulder at about 460 nm which is assigned to $^4T_{1g}(F) \rightarrow {}^4A_{2g}(F)$ transition that is manifold splitted due to multiplet coupling. The strategy adopted in this study can extended to explore more organically-template metal pyrophosphates with interesting structural topology.

Acknowledgments

Funding by the DFG (German Research Foundation) for David Bauer is gratefully acknowledged.

Competing Interests

The authors declare that they have no competing interests.

Authors Contributions Statement

Alaoui Tahiri synthesized the phosphate and wrote the manuscript. El Bali planned the characterizations and led the submitted manuscript to its final version. Dr Wilson solved the crystal structure and contributed to the description of the crystal structure. Prof. Lachkar contributed also to

the corrections. Dr Bower and Prof. Haisch measured the IR, Raman and UV-Vis spectra and contributed to the corrections of their part.

Figures and Tables Caption

Figure 1: The asymmetric unit in $[Co(H_2P_2O_7)_2(H_2O)_2][(CH_3)_3C\text{-}NH_3)_2].2H_2O$.

Figure 2: Projection onto (100) of the crystal structure of $[Co(H_2P_2O_7)_2(H_2O)_2][(CH_3)_3C\text{-}NH_3)_2].2H_2O$. Dashed lines are the H-bonds network.

Figure 3: IR of $[Co(H_2P_2O_7)_2(H_2O)_2][(CH_3)_3C\text{-}NH_3)_2].2H_2O$. **Figure 4**: Average Raman spectrum (blue line) of 13 single spectra (light blue) collected from different spots of several single crystals using a 20x objective, 532 nm laser with 1 mW laser power, 5 s integration time and 3 accumulations.

Figure 5: Uv-Vis spectrum of $[Co(H_2P_2O_7)_2(H_2O)_2][(CH_3)_3C\text{-}NH_3)_2].2H_2O$.

Table 1: Crystal data and structure refinement for $[Co(H_2P_2O_7)_2(H_2O)_2][(CH_3)_3C\text{-}NH_3)_2].2H_2O$.

Table 2: Atomic coordinates and equivalent isotropic displacement parameters U(eq) for $[Co(H_2P_2O_7)_2(H_2O)_2][(CH_3)_3C\text{-}NH_3)_2].2H_2O$.

Table 3a: Main interatomic distances (Å) and bond angles (°) in the $[CoO_6]$ octahedron.

Table 3b: Main interatomic distances (Å) and bond angles (°) in the HP_2O_7 group in $[Co(H_2P_2O_7)_2(H_2O)_2][(CH_3)_3C\text{-}NH_3)_2].2H_2O$.

Table 4: I.R. and Raman bands assignments for $[Co(H_2P_2O_7)_2(H_2O)_2][(CH_3)_3C\text{-}NH_3)_2]\cdot H_2O$.

References

[1] Z. Xiao, Y. Sun, Y. Xiang, B. Yuexin, S. Rujie, Z.L. Wang, Two new inorganic–organic hybrid zinc phosphate frameworks and their application in fluorescence sensor and photocatalytic hydrogen evolution, J. Sol. State Chem. 269 (2019) 575-579. https://doi.org/10.1016/j.jssc.2018.10.038.

[2] J.L. Song, J.H. Zhang, J.G. Mao, Non-noble metal vanadium phosphites with broad absorption for photocatalytic hydrogen evolution, J. Sol. State Chem. 237 (2016) 371-377. https://doi.org/10.1016/j.jssc.2016.02.035.

[3] S.K. Lee, U.H. Lee, Y.K. Hwang, J.S. Chang, N.H. Jang, Catalytic and sorption applications of porous nickel phosphate materials, Catal. Today. 324 1 (2019) 154-166. https://doi.org/10.1016/j.cattod.2018.06.012.

[4] J. Huang, J. Cai, C.M. Li, X.K. Fu, A series of crystalline organic polymer–inorganic hybrid material zinc-phosphonate-phosphates synthesized in the presence of templates for superior performance catalyst support, Inorg. Chem. Comm. 48 (2014) 36-39. https://doi.org/10.1016/j.inoche.2014.08.006.

[5] S. Natarajan, M. Eswaramoorthy, C.N.R. Rao, S. Natarajan, A.K. Cheetham, A three-dimensional open-framework tin(II) phosphate exhibiting reversible dehydration and ion-exchange properties, Chem. Commun. 15 (1998) 1561-1562. https://doi.org/10.1039/A802478B.

[6] S. Fernández, J.L.Mesa, J.L.Pizarro, A. Peña, J. Gutiérrez, M.I. Arriortua, T. Rojo, Magnetic behavior of inorganic–organic hybrid phosphite compounds with 3d transition metals, J. Magn. Magn. Mater. 272–276 2 (2004) 1113-1115. https://doi.org/10.1016/j.jmmm.2003.12.042.

[7] Ann M. Chippindale, F.O.M. Gaslain, A.R. Cowley, A.V. Powell, Synthesis and characterisation of a layered organically-templated manganese phosphate $[Mn_2(HPO_4)_3]\cdot(NH_3(CH_2)_2NH_3)_{3/2}\cdot H_2PO_4$, and its reaction with water, J. Mater. Chem. 11 (2001) 3172-3179. https://doi.org/10.1039/B104491P.

[8] G. Li, Y. Xing, S. Song, Synthesis, structures and magnetic properties of two new one-dimensional cobalt (II) phosphites with organic amines acting as ligands, J. Sol. State Chem. 181 4 (2008) 943-949. https://doi.org/10.1016/j.jssc.2008.01.043.

[9] N. Hamdi, S. Chaouch, I. da Silva, M. Ezahri, M. Lachkar, R. Alhasan, A. Yaman Abdin, C. Jacob, B. El Bali, Synthesis, Structural Characterization, and Biological Activities of Organically

Templated Cobalt Phosphite $(C_4N_2H_{14})Co(H_2PO_3)_4{\cdot}2H_2O$, Sci. 1 (2019) 13. https://doi.org/10.3390/sci1010013.v1.

[10] C.N.R. Rao, S. Natarajan, A. Choudhury, S. Neeraj, A.A. Ayi, Aufbau Principle of Complex Open-Framework Structures of Metal Phosphates with Different Dimensionalities, Acc. Chem. Res. 34 1 (2001) 80-87. https://doi.org/10.1021/ar000135+.

[11] L.M. Li, K. Cheng, J. Zhang, An inorganic–organic hybrid zinc phosphite framework with unusual topology, Inorg. Chem. Comm. 30 (2013) 136–138. https://doi.org/10.1016/j.inoche.2013.02.008.

[12] X. Jing, L. Zhang, S. Gong, G. Li, M. Bi, Q. Huo and Y. Liu, Hydrothermal synthesis and characterization of two novel three-dimensional vanadium phosphites: $|(C_{10}H_{10}N_2)|[V^{IV}_2O_2(HPO_3)_2(H_2PO_3)_2]$ and $|(C_4H_{16}N_3)|[V^{IV}_2V^{III}O_2F_2(HPO_3)_4$, Micropor. Mesopor. Mat. 116 (2008) 101–107. https://doi.org/10.1016/j.micromeso.2008.03.026.

[13] G. Zhou, Y. Yang, R. Fan, X. Liu, H. Hong, F. Wang, Hydrothermal synthesis and characterization of a new organically templated three-dimensional open-framework gallium phosphate–phosphite $(C_6N_2H_{18})_2(C_6N_2H_{17})Ga_{15}(OH)_8(PO_4)_2(HPO_4)_{12}(HPO_3)_6{\cdot}2H_2O$, Sol. State Sci. 12(7) (2010) 1103-1106. https://doi.org/10.1016/j.solidstatesciences.2010.04.013.

[14] J. Li, T. Li, H. Zeng, G. Zou, Z. Lin, Solvent-free synthesis of inorganic-organic hybrid solids with chainlike, layered, and open-framework structures, Inorg. Chem. Comm. 95 (2018) 8-11. https://doi.org/10.1016/j.inoche.2018.06.022.

[15] G.M. Wang, X. Zhang, J.H. Li, Z.H. Wang, Y.X. Wang, J.H. Lin, A new hybrid zinc phosphite with a pillared layered structure: Synthesis and characterization of $[C_6N_2O_2H_{16}][Zn(HPO_3)]_2$, Inorg. Chem. Comm. 36 (2013) 27-30. https://doi.org/10.1016/j.inoche.2013.08.008.

[16] G.M. Wang, J.H. Li, C.L. Gao, J.C. Zhang, X. Zhang, Z.Z. Bao, Y.X. Wang, J.H. Lin, Synthesis and characterization of a novel inorganic–organic hybrid open-framework zinc phosphate with 16-ring channels, Solid State Sci. 39 (2015) 1-5. https://doi.org/10.1016/j.solidstatesciences.2014.11.007.

[17] X. Zhang, X. Li, J. Zhang, Solvothermal synthesis, crystal structures and characterization of open-framework metal (Co(II) and Mn(II)) phosphites with helical channels and 16-membered rings, Inorg. Chem. Comm. 84 (2017) 77-80. https://doi.org/10.1016/j.inoche.2017.07.022.

[18] L. Liu, W. Zhang. Z. Shi. Y. Chen, Z. Lin, Solvent-free synthesis of new metal phosphites with double-layered, pillared-layered, and framework structures, Sol. State Sci. 38 (2014) 13-17. https://doi.org/10.1016/j.solidstatesciences.2014.09.013.

[19] G.M. Wang, J.Q. Jiao, X. Zhang, X.M. Zhao, X. Yin, Z.H. Wang, Y.X. Wang, J.H. Lin, Syntheses and characterizations of zinc phosphites with new templates generated by N-alkylation transformations, Inorg. Chem. Comm. 39 (2014) 94-98. https://doi.org/10.1016/j.inoche.2013.11.013.

[20] G.M. Wang, J.H. Li, J.Q. Jiao, X. Zhang, X.M. Zhao, X. Yin, J.S. Huang, Y.X. Wang, J.H. Lin, Synthesis and structural characterization of two open-framework zinc phosphites with (3,4)-connected networks, Inorg. Chem. Comm. 43 (2014) 105-109. https://doi.org/10.1016/j.inoche.2014.02.023.

[21] A. Ben Rached, W. Maalej, P. Guionneau, N. Daro, T. Mhiri, H. Feki, Z. Elaoud, Synthesis, crystal structure, and vibrational and DFT simulation studies of benzylammonium dihydrogen phosphite, J. Phys. Chem. Solids. 123 (2018) 150-156. https://doi.org/10.1016/j.jpcs.2018.07.017.

[22] M.A. Salvadó, P. Pertierra, C. Trobajo, J.R. García, Supramolecular open-framework based on 1-D iron phosphate–diphosphate chains assembled through hydrogen bonding, J. Sol. State Chem. 181(5) (2008) 1103-1109. https://doi.org/10.1016/j.jssc.2008.02.012.

[23] R. Essehli, B. El Bali, M. Lachkar, M. Dusek, K. Fejfarova, M. Bolte, $(C_2N_2H_{10})_2Mg(HP_2O_7)_2{\cdot}2H_2O$ synthesis and crystal structure, J. Chem. Crystallogr. 36(10) (2006) 655–660. https://doi.org/10.1007/s10870-006-9113-5.

[24] F. Capitelli, B. El Bali, R. Essehli, M. Lachkar, V. Valentini, G. Mattei, J. Taraba, Z. Zak, New isostructural ethylenediammonium diphosphates $(NH_3(CH_2)_2NH_3)_2[Me(HP_2O_7)_2{\cdot}2H_2O]$ [Me= Co, Ni]: X-ray crystal structure and vibrational spectroscopy, Z. Kristallogr. 221 (2006) 649–655. https://doi.org/10.1524/zkri.2006.221.9.649.

[25] F. Capitelli, B. El Bali, R. Essehli, M. Lachkar, I. da Silva, New hybrid diphosphates Ln(2)($NH_2(CH_2)(2)NH_2$)(HP_2O_7)(2)center dot 4H(2)O (Ln=Eu, Tb, Er): synthesis, single crystal and powder X-ray crystal structure, Z. Kristallogr. 221 (2006) 788–794. https://doi.org/10.1524/zkri.2006.221.12.788.

[26] Y. He, Y. Yan, F. Yang, J. Wu, X. Song, Ionothermal synthesis of a new open-framework manganese(II) diphosphate, Inorg. Chem. Comm. 44 (2014) 151–154. https://doi.org/10.1016/j.inoche.2014.03.024.

[27] E. Zito, T. J. Greenfield, J. Minichelli, M. Nanao, M.M. Turnbull, R.P. Doyle, J. Zubieta, Synthesis, structure and magnetic properties of a binuclear Co(II)-pyrophosphate complex, [Co_2(phenanthroline-dione)$_4$(P_2O_7)], Polyhedron 170 (2019) 705-711. https://doi.org/10.1016/j.poly.2019.06.039.

[28] A.T. Alaoui, R. Ouarsal, M. Lachkar, B. El Bali, M. Bolte, Cobalt potassium dihydrogendiphosphate dihydrate, $CoK_2(H_2P_2O_7)_2{\cdot}2H_2O$, Acta Cryst. E58 (2002) i91-i92. https://doi.org/10.1107/S1600536802016161.

[29] A.T. Alaoui, R. Ouarsal, M. Lachkar, P.Y. Zavalij, B. El Bali, Dipotassium manganese(II) bis(dihydrogendiphosphate) dihydrate, $K_2Mn(H_2P_2O_7)_2{\cdot}2H_2O$, Acta Cryst. E59 (2003) i68-i69. https://doi.org/10.1107/S1600536803007189.

[30] A.T. Alaoui, I. Messouri, M. Lachkar, P.Y. Zavalij, R. Glaum, B. El Bali, R. Ouarsal, Dipotassium nickel(II) bis(dihydrogendiphosphate) dihydrate, $K_2Ni(H_2P_2O_7)_2{\cdot}2H_2O$, Acta Cryst. E60 (2004) i3-i5. https://doi.org/10.1107/S1600536803028344.

[31] A.T. Alaoui, R. Ouarsal, M. Lachkar, P.Y. Zavalij, B. El Bali, Dipotassium zinc bis(dihydrogendiphosphate)dihydrate, $K_2Zn(H_2P_2O_7)_2{\cdot}2H_2O$, Acta Cryst. E59 (2003) i50-i52. https://doi.org/10.1107/S1600536803005440.

[32] R. Essehli, B. El Bali, A.T. Alaoui, M. Lachkar, B. Manoun, M. Dusek, K. Fejfarova, $K_2M(H_2P_2O_7)_2{\cdot}2H_2O$ (M: Ni, Cu, Zn): Orthorhombic forms and Raman Spectra, Acta Cryst. C61 (2005) i120-i124. https://doi.org/10.1107/S0108270105036656.

[33] R. Essehli, B. El Bali, M. Lachkar, G. Cruciani, Two new acidic diphosphates $Rb_2M(H_2P_2O_7)_2{\cdot}2H_2O$ (M = Zn and Mg): Crystal Structures and vibrational study, J. Alloys Compd. 492 (2010) 358-362. https://doi.org/10.1016/j.jallcom.2009.11.095.

[34] R. Essehli, M. Lachkar, I. Svoboda, H. Fuess, B. El Bali, Synthesis, crystal structure and vibrational spectra of a new diammonium zinc(II) di-hydrogendiphosphate dihydrate, $(NH_4)_2Zn(H_2P_2O_7)_2{\cdot}2H_2O$, Acta Cryst, E61 (2005) i32-i34. https://doi.org/10.1107/S1600536805004642.

[35] R. Essehli, M. Lachkar, I. Svoboda, H. Fuess, B. El Bali, $(NH_4)_2[Co(H_2P_2O_7)_2(H_2O)_2]$, Acta Cryst. E61 (2005) i61-i63. https://doi.org/10.1107/S1600536805008639.

[36] R. Essehli, M. Lachkar, I. Svoboda, H. Fuess, B. El Bali, $(NH_4)_2[Ni(H_2P_2O_7)_2(H_2O)_2]$, Acta Cryst. E61 (2005) i64-i66. https://doi.org/10.1107/S1600536805008640.

[37] B. El Bali, F. Capitelli, A.T. Alaoui, M. Lachkar, I. da Silva, A. Alvarez-Larena, J. F. Piniella, New thallium diphosphates $Tl_2Me(H_2P_2O_7)_2 \cdot 2H_2O$, Me = Mg, Mn, Co, Ni and Zn. Synthesis, single crystal X-ray structures and powder X-ray structure of the Mg phase, Z. Kristallogr. 223 (2008) 448–455. https://doi.org/10.1524/zkri.2008.0047.

[38] G.M Sheldrick, Crystal structure refinement with SHELXL, Acta Cryst. C71 (2015) 3-8. https://doi.org/10.1107/S2053229614024218.

[39] G.M. Sheldrick, A short history of SHELX, Acta Cryst. A64 (2008) 112–122. https://doi.org/10.1107/S0108767307043930.

[40] O.V. Dolomanov, L.J Bourhis, R.J. Gildea, J.A. Howard, H. Puschmann, OLEX2: a complete structure solution, refinement and analysis program, J. Appl. Cryst. 42 (2009) 339-341. https://doi.org/10.1107/S0021889808042726.

[41] K. Brandenburg K, H. Putz, (2005), DIAMOND. Version 3. Crystal Impact GbR, Bonn, Germany.

[42] M.E. Fleet, Distortion parameters for coordination polyhedra, Mineral. Mag. 40 (1976) 531-533. https://doi.org/10.1180/minmag.1976.040.313.18.

[43] K. Robinson, G.V. Gibbs, P.H. Ribbe, Quadratic elongation: a quantitative measure of distortion in coordination polyhedral, Science 172 (1971) 567-570. https://doi.org/10.1126/science.172.3983.567.

[44] F.A. Itoua Ngopoh, M. Lachkar, T. Dordević, C. L. Lengauer, B. El Bali, Synthesis, Crystal Structure and Characterization of a 2D-hybrid Cobalt Hypophosphite, J. Chem. Crystallogr. 45 (2015) 369-375. https://doi.org/10.1007/s10870-015-0603-1.

[45] P.K. Kipkemboi, P.C. Kiprono, J.J. Sanga, Vibrational spectra of t-butylalcohol, t-butylamine and t-butylalcohol+t-butylamine binary liquid mixtures, Bull. Chem. Soc. Ethiop. 17 (2) (2003) 211-218. https://doi.org/10.4314/bcse.v17i2.61689.

[46] R. L. Frost, Y. Xi, Molecular structure of the phosphate mineral brazilianite $NaAl_3(PO_4)_2(OH)_4$ – A semi precious jewel, J. Mole. Structure. 1010 (2012) 179-183. https://doi.org/10.1016/j.molstruc.2011.12.003

[47] A.A. Belik, H-J. Koo, M-H. Whangbo, N. Tsujii, P. aumov and E. Takayama-Muromachi., Magnetic Properties of Synthetic Libethenite Cu_2PO_4OH: a New Spin-Gap System., Inorg. Chem. 46(21) (2007) 8684–8689., https://doi.org/10.1021/ic7008418.

[48] B.Bazán, J.L.Mesa, J.L. Pizarro, M.I.Arriortua, T. Rojo, Hydrothermal synthesis, crystal structure, and spectroscopic characterization of a new organically templated mixed-anion fluoro-arsenate-phosphate iron(III) compound, $(C_2H_{10}N_2)[Fe_2(AsO_4)_2{-}x(PO_4)_xF_2(H_2O)]$ (x = 0.46)., Mat. Res. Bull. 38 7 (2003) 1193-1202. https://doi.org/10.1016/S0025-5408(03)00106-5

[49] K.D. Litasov, N.M. Podgornykh, Raman spectroscopy of various phosphate minerals and occurrence of tuite in the Elga IIE iron meteorite, *J. Raman Spectroscopy.*, *48*(11) (2017) 1518-1527. https://doi.org/10.1002/jrs.5119.

[50] M.S. Idrissi, L. Rghioui, R. Nejjar, L. Benarafa, M. S. Idrissi, A. Lorriaux, F. Wallart,

Spectres de vibration des diphosphates monocliniques de formule AMP_2O_7, Spectrochim. Acta A,

Molecular and biomolecular spectroscopy. 60 (2004) 2043-2052.

https://doi.org/10.1016/j.saa.2003.11.002.

[51] J-C. Ballhausen, Introduction to ligand field theory, (1962) McGraw-Hill, New York.

[52] B. N. Figgis, Michael A. Hitchman., Ligand Field Theory and Its Applications, (2000) New

York: Wiley-VCH.

Table 1. Crystal data and structure refinement for $[Co(H_2P_2O_7)_2(H_2O)_2][(CH_3)_3C\text{-}NH_3]_2 \cdot 2H_2O$

Chemical formula	$[Co(H_2P_2O_7)_2(H_2O)_2][(CH_3)_3C\text{-}NH_3]_2 \cdot 2H_2O$
Formula weight (g/mol)	631.20
Temperature (K)	295
Wavelength ($\lambda_{K\alpha}$, Å)	0.71073
Crystal system, space group	Orthorhombic, Cmce (# 64)
Unit cell dimensions (Å)	a = 11.9 642(10), b = 9.1565(8), c = 24.488(2)
Volume ($Å^3$), Z	2682.7(4), 4
F(000), Absorption coefficient (mm^{-1})	1316, 0.953
Tmin / Tmax	0.878 / 0.911
Crystal sizes (mm)	0.14*0.12*0.10
θ–range (°)	2.922-28.304
Limiting indices	$-15 \leq h \leq 13$, $-12 \leq k \leq 12$, $-32 \leq l \leq 29$
Reflections collected / reflections with $I > 2\sigma(I)$ / parameters	1723/1520/105
$R[F2 > 2\sigma(F2)]$ / $wR(F2)$	0.0396 / 0.0912

w=1/[\s^2^(Fo^2^)+(0.0538P)^2^+2.0458P] where P=(Fo^2^+2Fc^2^)/3

Table 2. Atomic coordinates and equivalent isotropic displacement parameters U(eq) for $[Co(H_2P_2O_7)_2(H_2O)_2][(CH_3)_3C\text{-}NH_3]_2 \cdot 2H_2O$

Atom	x	y	z	Uani
Co1	0.000000	1.000000	0.500000	0.02039(15)
P1	-0.25203(4)	0.96385(5)	0.44166(2)	0.02416(15)
O1	-0.12905(10)	0.94107(15)	0.44549(5)	0.0282(3)
O2	-0.30086(19)	1.000000	0.500000	0.0742(11)
O3	-0.31895(10)	0.83799(14)	0.42041(6)	0.0310(3)
O4	-0.28268(15)	1.09680(17)	0.40606(10)	0.0588(6)
H4	-0.245(2)	1.173(3)	0.4103(14)	0.073(10)
O1W	0.000000	1.2150(2)	0.47546(11)	0.0403(6)

H1W	-0.054(2)	1.251(4)	0.4604(12)	0.057(8)
N1	0.000000	0.7642(3)	0.37318(11)	0.0328(5)
H1A	0.0578(19)	0.788(3)	0.3924(11)	0.044(7)
H1B	0.000000	0.672(5)	0.3727(15)	0.048(11)
C1	0.000000	0.8311(4)	0.31720(12)	0.0434(7)
C2	-0.1049(2)	0.7792(4)	0.28847(12)	0.0708(9)
H2A	-0.107718	0.820010	0.252394	0.106
H2B	-0.104145	0.674513	0.286091	0.106
H2C	-0.169437	0.810029	0.308742	0.106
C3	0.000000	0.9964(5)	0.32386(19)	0.0765(15)
H3A	0.015872	1.041462	0.289333	0.115
H3B	0.056121	1.023992	0.349904	0.115
H3C	-0.071993	1.027843	0.336550	0.115
O2W	0.000000	0.4500(3)	0.35098(11)	0.0463(6)
H2W	-0.054(3)	0.413(5)	0.3643(17)	0.108(15)

Table 3a. Main interatomic distances (Å) and bond angles (deg) in the [CoO_6] octahedron.

Co	**O1**	**O1^{i}**	**O1^{ii}**	**O1^{iii}**	**O1w**	**O1w^{i}**
O1	**2.111(1)**	2.880(2)	3.088(2)	4.222(2)	3.035(2)	2.859(2)
O1^{i}	86.00(5)	**2.111(1)**	4.222(2)	3.088(2)	2.859(2)	3.035(2)
O1^{ii}	180.00(5)	94.00(5)	**2.111(1)**	2.880(2)	2.859(2)	3.035(2)
O1^{iii}	94.00(5)	180.00(5)	86.00(5)	**2.111(1)**	3.035(2)	2.859(2)
O1w	93.43(4)	86.57(4)	93.43(4)	86.57(4)	**2.058(2)**	4.117(3)
O1w^{i}	86.57(4)	93.43(4)	86.57(4)	93.43(4)	180.00(5)	**2.058(2)**

Table 3b. Main interatomic distances (Å) and bond angles (deg) in the HP_2O_7 group in $[Co(H_2P_2O_7)_2(H_2O)_2][(CH_3)_3C\text{-}NH_3]_2 \cdot 2H_2O$

P1—O2—P1^{i} **Tetrahedron around P(1)**				
P1	O1	O2	O3	O4
O1	**1.489(1)**	2.510(2)	2.536(2)	2.519(2)
O2	109.76(6)	**1.579(1)**	2.459(1)	2.475(2)
O3	116.27(7)	106.15(6)	**1.497(1)**	2.435(2)
O4	112.41(9)	112.41(9)	104.96(9)	**1.542(1)**

Symmetry codes: ^{i} : x, 2-y, 1-z ; ^{ii} : 1-x, y, z ; ^{iii} : -x, 2-y, 1-z

Table 4. I.R. and Raman bands assignments for $[Co(H_2P_2O_7)_2(H_2O)_2][(CH_3)_3C\text{-}NH_3)_2]\cdot H_2O$

I. R.	Raman	Assigned mode
3463	3466	$\nu(H_2O)$
	3460 3390 3300 3200 3115	$\nu_s(NH_3^+)$ + $\nu_{as}(NH_3^+)$
	2980 2972 2950 2922	$\nu_s(CH_3)$ + $\nu_{as}(CH_3)$
2390 2370	2880 2780	
1840 1820 1590 1546 1460 1429 1359	 1720 1615 1526 1470	$\delta(OH)$ + $\delta_s(NH_3^+)$ + $\delta_{as}(NH_3^+)$ $\delta_s(CH_3)$ + $\delta_{as}(CH_3)$
1280	1270 1230	CC_4 skeletal streching C_3C-N streching
1186 1164 1009 980	 1054 990	$\nu_s(PO_3)$ + $\nu_s(PO_3)$
910	931 862	$\nu_{as}(POP)$
750	736	$\nu_s(POP)$
----	580 530 469	$\rho(H_2O)$ + $\delta(PO_3)$

		+ $\rho(PO_3)$

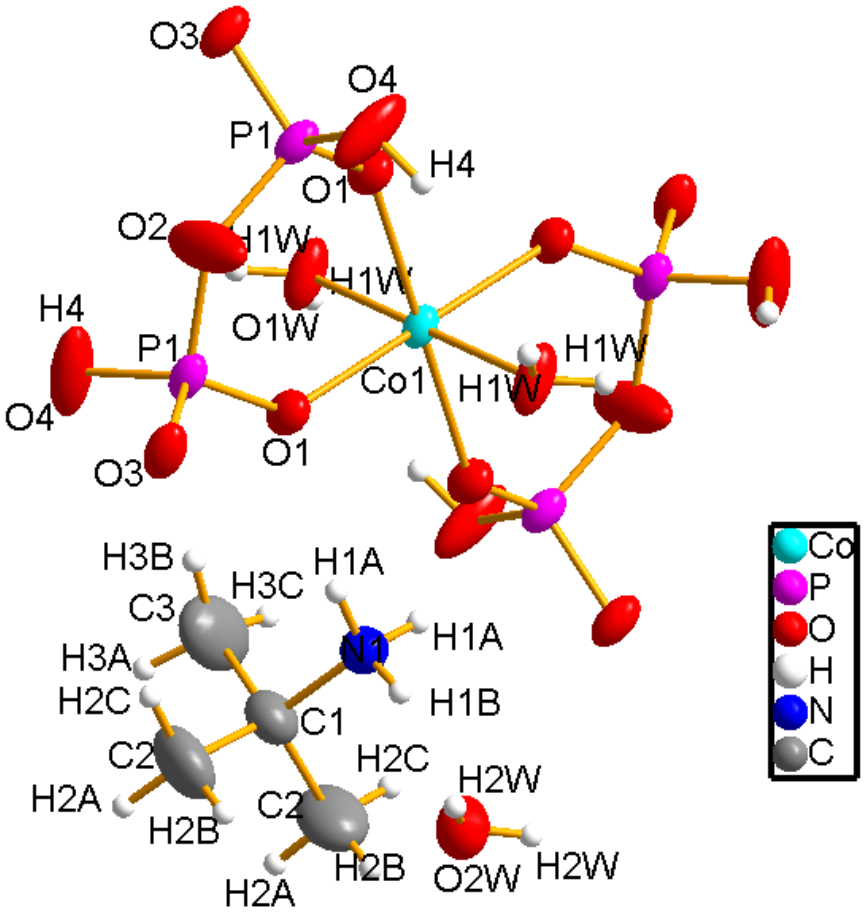

Figure 1: The asymmetric unit in $[Co(H_2P_2O_7)_2(H_2O)_2][(CH_3)_3C\text{-}NH_3)_2]\cdot 2H_2O$

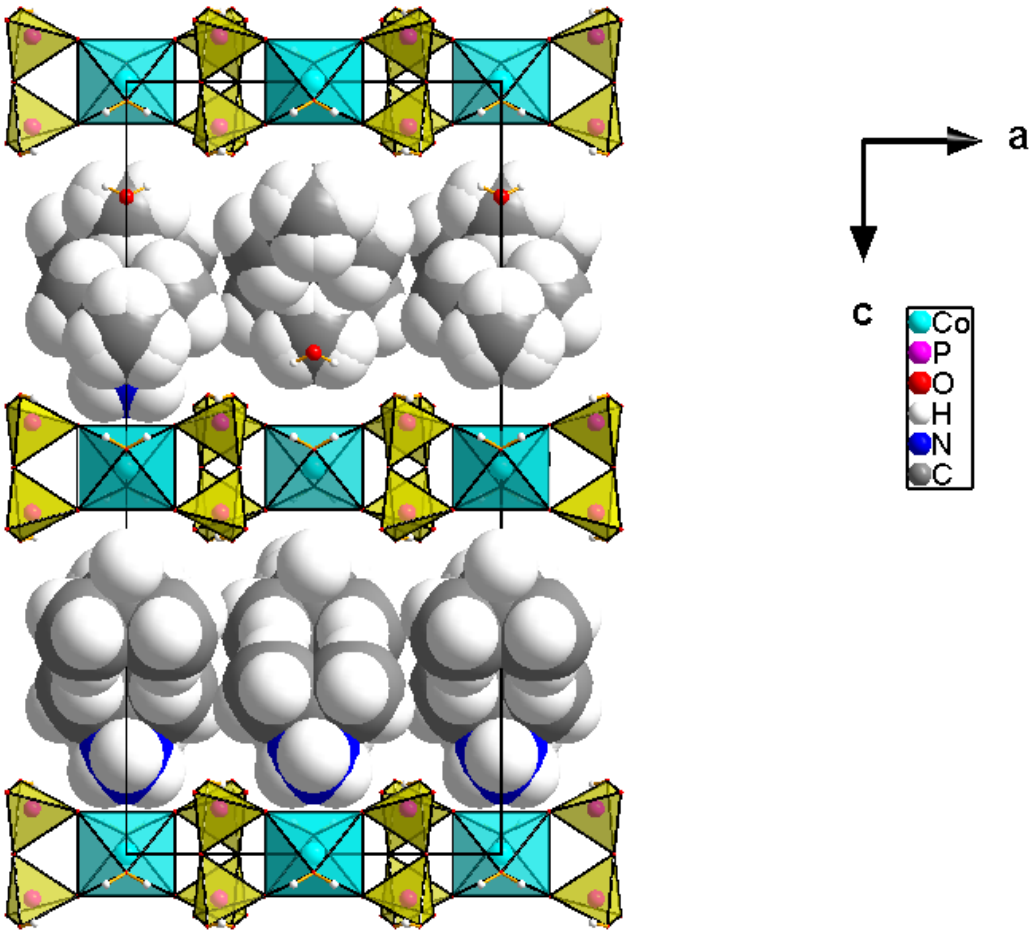

Figure 2: Projection onto *ac*-plane of the crystal structure of $[Co(H_2P_2O_7)_2(H_2O)_2][(CH_3)_3C\text{-}NH_3)_2]\cdot 2H_2O$.

Figure 3: IR of $[Co(H_2P_2O_7)_2(H_2O)_2][(CH_3)_3C\text{-}NH_3)_2]\cdot 2H_2O$.

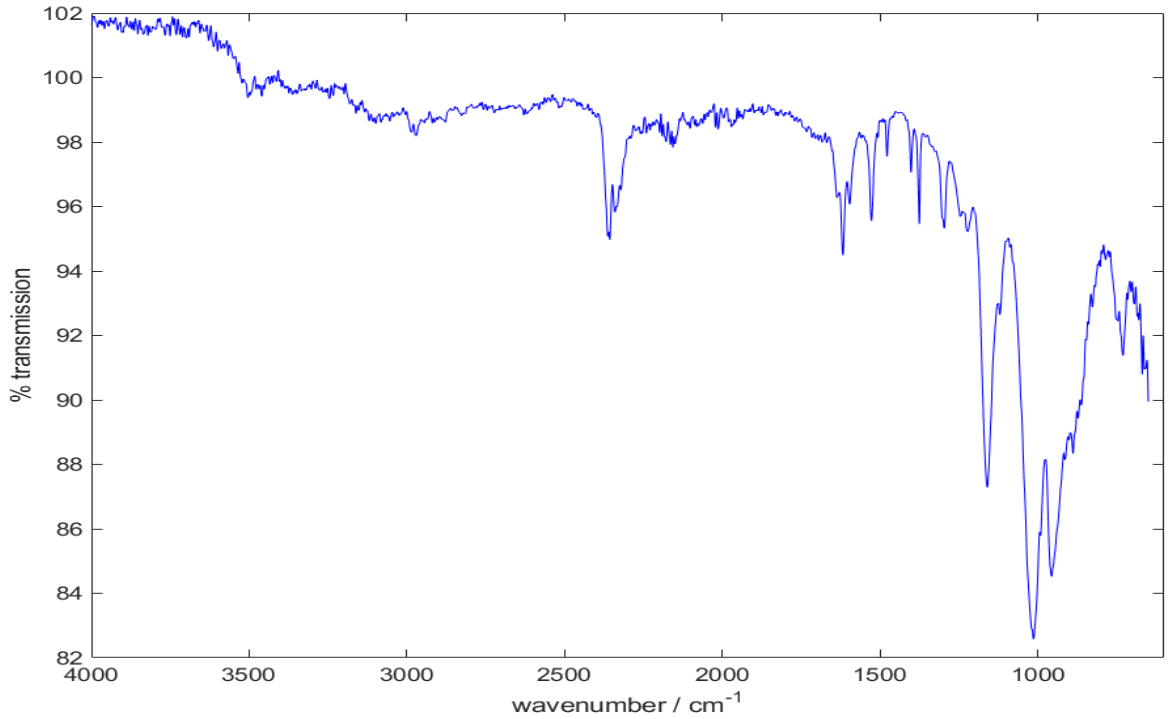

Figure 4: Average Raman spectrum (blue line) of 13 single spectra (light blue) collected from different spots of several single crystals using a 20x objective, 532 nm laser with 1 mW laser power, 5 s integration time and 3 accumulations.

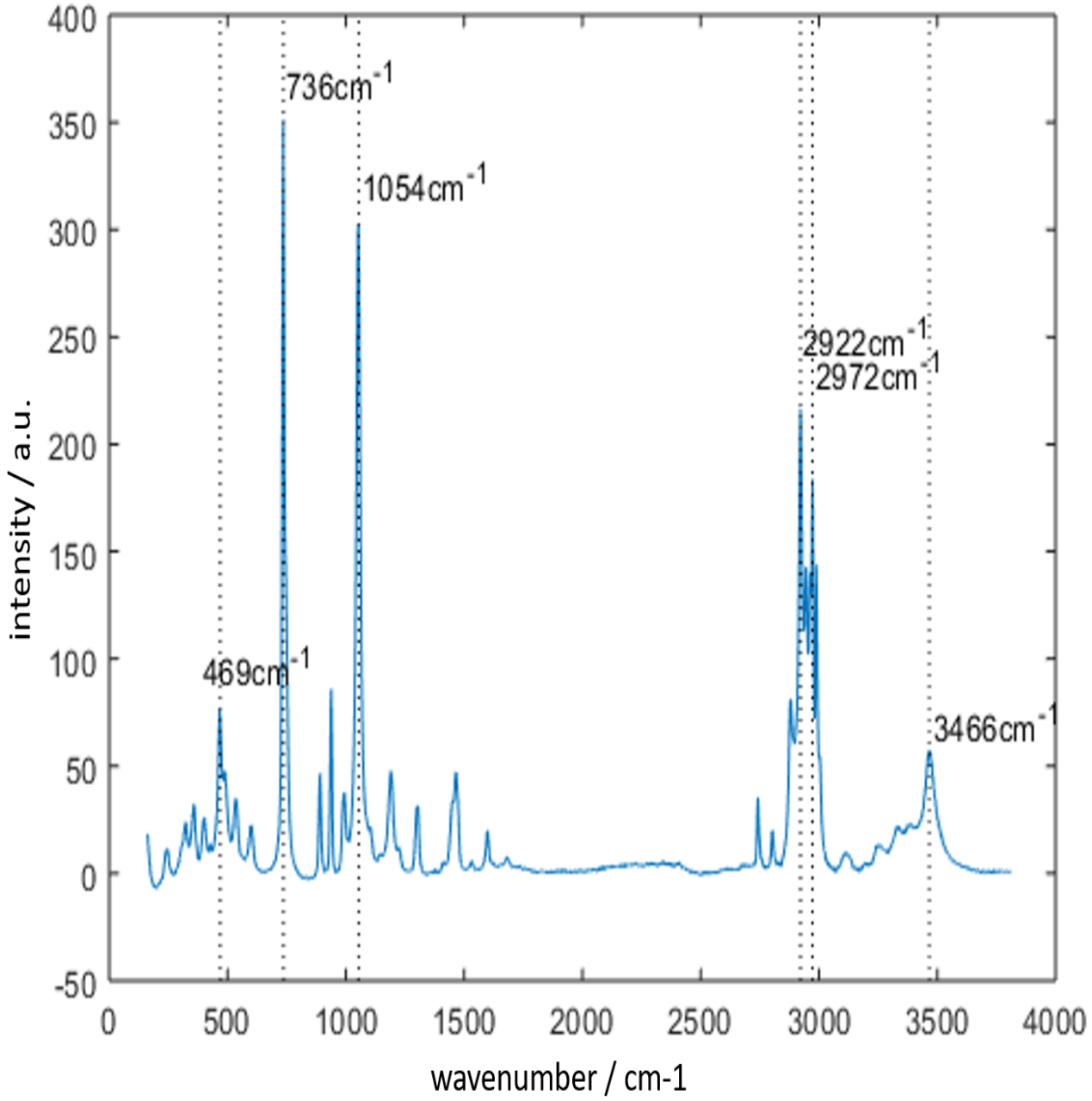
736cm-1
1054cm-1
2922cm-1
2972cm-1
469cm-1
3466cm-1
intensity / a.u.
wavenumber / cm-1
400
350
300
250
200
150
100
50
0
-50
0
500
1000
1500
2000
2500
3000
3500
4000

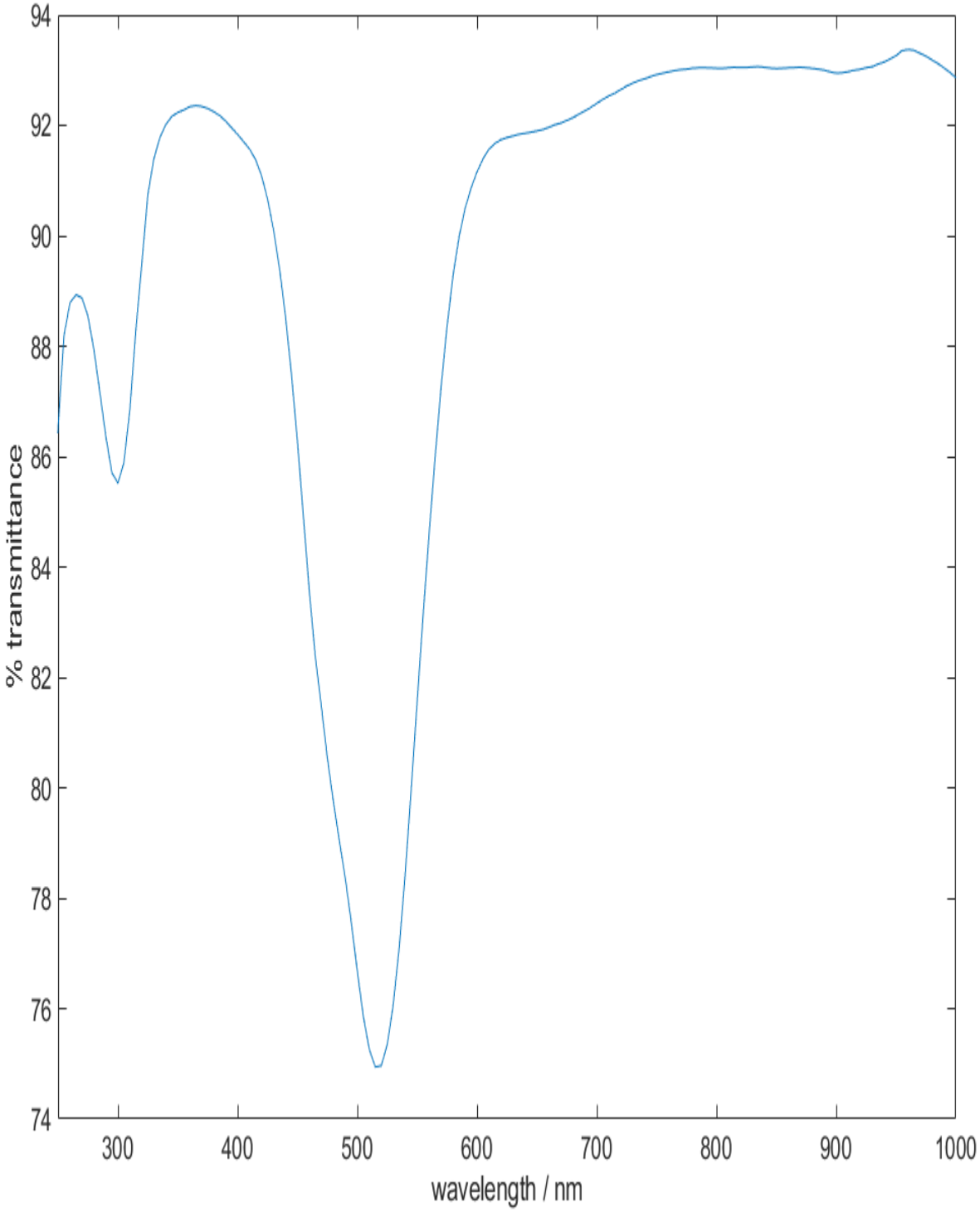

Figure 5: Uv-Vis spectrum of $[Co(H_2P_2O_7)_2(H_2O)_2][(CH_3)_3C\text{-}NH_3)_2].2H_2O$.

The authors of this publication: *Aziz Alaoui Tahiri, Brahim El Bali, Mohammed Lachkar, Claire Wilson, David Bauer and Christoph Haisch***, declare no conflict of interest at all.**

Highlights

- $[Co(H_2P_2O_7)_2(H_2O)_2][(CH_3)_3C\text{-}NH_3]_2 \cdot 2H_2O$ a new hybrid phosphate is reported.
- IR spectroscopy confirmed the existence of the phosphate group P_2O_7.
- Five 4*f*–4*f* ascribed absorption bands are observed in the UV-NIR fields.

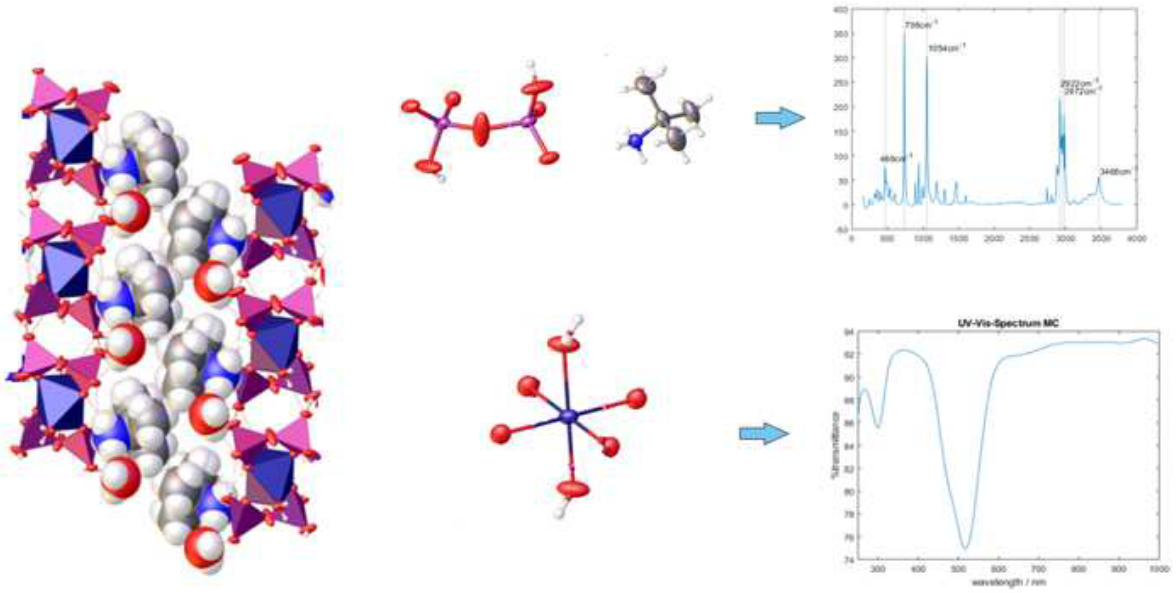
UV-Vis-Spectrum MC
%transmittance
wavelength / nm